PIN versus PN Homojunctions in GaInAsSb 2.0-2.5 Micron Mesa Photodiodes

J. P. Prineas[a,b], J.R. Yager[a,b], J. T. Olesberg[b,c], S. Seydmohamadi[a,b], C. Cao[a,b], M. Reddy[b], C. Coretsopoulos[b], J. L. Hicks[a,b], T.F. Boggess[a,b], M. Santilli[d], L.J. Olafsen[d]

[a]Department of Physics and Astronomy, University of Iowa, Iowa City, IA, USA 52242
[b]Optical Science and Technology Center, University of Iowa, Iowa City, IA, USA 52242
[c]Department of Chemistry, University of Iowa, Iowa City, IA, USA 52242
[d]Department of Physics and Astronomy, Kansas University, Lawrence, KS, USA 66045-7582

ABSTRACT

The performances of a pin versus a pn structure from GaInAsSb materials operating at room temperature are compared both from a theoretical point of view and experimentally. Theoretically, it is found in materials limited by generation-recombination currents, pn junctions have a higher D* than pin junctions. The thinner depletion region of pn junctions results in a lower responsivity but a higher dynamic resistance, giving an overall higher D* compared to a pin structure. A series of five p+pn+ $Ga_{0.80}In_{0.20}As_{0.18}Sb_{0.82}$ detector structures latticed matched to GaSb substrates and with 2.37 μm cut off wavelength were grown by molecular beam epitaxy and processed into variable size mesa photodiodes. Only the doping of the absorbing (p) region was varied from sample to sample, starting with nominally undoped (~$1x10^{16}$ cm^{-3} p-background doping due to native defects) and increasing the doping until a p+n+ structure was attained. Room temperature dynamic resistance-area product R_0A was measured for each sample. A simple method is presented and used to disentangle perimeter from areal leakage currents. All five samples had comparable R_0A's. Maximum measured R_0A was 30 Ω-cm^2 in the largest mesas. Extracted R_0A's in the zero perimeter/area limit were about ~50 Ω-cm^2 (20-100 Ω-cm^2) for all samples. Within uncertainty, no clear trend was seen. Tentative explanations are proposed.

Keywords: pin photodiode, pn photodiode, quaternary materials, molecular beam epitaxy, GaInAsSb, GaSb, perimeter leakage

1. INTRODUCTION

Pin and pn photodiodes fabricated from GaInAsSb quaternary materials operating in the 2.0-2.5 micron wavelength range have many important applications, including photodetectors for near-infrared spectroscopy of molecules and thermophotovoltaic devices for conversion of heat to electrical energy. We are interested in particular in continuous optical sensing of glucose concentrations in an aqueous solution, important for the treatment of diabetes. The bandgap of $Ga_xIn_{1-x}As_ySb_{1-y}$ can be continuously tuned from about 475 to 730 meV while remaining lattice-matched to a GaSb substrate[1], as shown in Fig. 1, and in contrast to leading ternary materials in this range such as InGaAs on InP. The spectral responsivity of GaInAsSb pin photodiodes can be optimized to glucose specific absorption features in the important combination spectral region[2], as shown in Fig. 2.

Pn detectors operate by photogeneration of a current of electrons and holes from the absorption of light within a diffusion length of the depletion region. From the depletion region, electrons and holes are accelerated to the n and p regions, respectively, where they are collected by the metal contacts. An important figure of merit used to describe pn detectors is the zero bias dynamic resistance, defined as $(R_0=dI/dV)^{-1}{}_{V=0}$, —mesa area (A) product R_0A. Together with spectral responsivity R_λ, defined as the Amps of current generated by the detector at zero bias voltage per Watt of incident light, these two important figures of merit characterize the D* of the detector, which is a measure of the S/N of the detector per unit incident radiation: $D^*(\lambda) = R_\lambda(R_0A/4k_BT)^{1/2}$, where k_B is the Boltzman constant and T is the temperature.

The usual expectation is that the spectral responsivity and hence the detectivity of a detector can be improved by increasing the thickness of the depletion region. In a true pin structure, the depletion region stretches across the entire i-

Semiconductor Photodetectors III, edited by Marshall J. Cohen, Eustace L. Dereniak, Proc. of SPIE Vol. 6119, 611903, (2006) · 0277-786X/06/$15 · doi: 10.1117/12.647109

region, as shown by the dashed lines in Fig. 4 for the corresponding pin structure in Fig. 3. However, MBE as well as MOCVD grown GaInAsSb has a background p-type character (~$1x10^{16}$ cm^{-3}) which been attributed to the formation of native defects and not impurities in the crystal, and hence while p+pn+ diode junctions can be grown, true pin diode junctions can not. The effect of even light doping of the absorbing region on the width of the depletion region is dramatic, as seen in Fig. 4: the bands are flattened across the absorption region, and the depletion region gets squashed up against the interface with the n-region. The heavier the background doping, the thinner the depletion region gets. But this is not necessarily detrimental to the device performance. Photoexcitation of electrons and holes in the p-type absorbing region results in minority electrons that fairly easily diffuse to the depletion region (encouraged by small electric fields) due to their high mobility, while less mobile holes are also collected by virtue of being the majority carrier. Furthermore, the narrowing of the depletion region can reduce the generation-recombination current, which is directly proportional to the width of the depletion region. A natural question that arises in this context: is there an optimal doping of the absorbing region, with doping varying from background levels up until the structure becomes simply a pn junction?

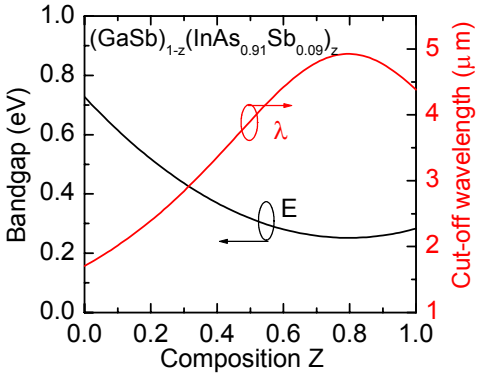

Fig. 1 The bandgap of $Ga_xIn_{1-x}As_ySb_{1-y}$ with x and y concentrations chosen in the ratio $(GaSb)_{1-z}(InAs_{0.91}Sb0.09)_z$ can be tuned continuously from about 475 to 730 meV while remaining lattice matched to a GaSb substrate.

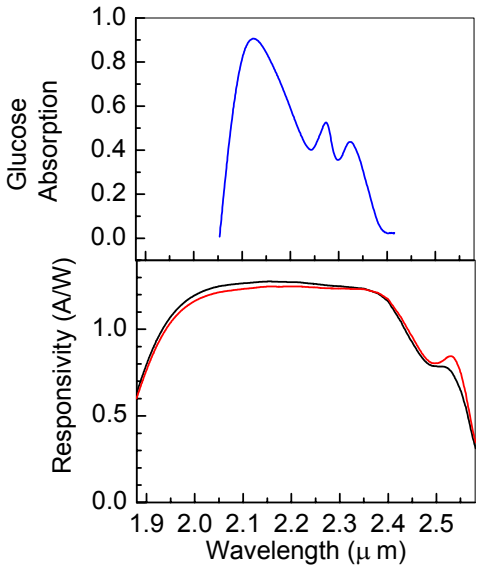

Fig. 2 The spectral responsivity of GaInAsSb can be well matched to an glucose specific absorption feature in the important combination spectral region as seen at top. Bottom plot shows the spectral response of $Ga_{0.79}In_{0.21}As_{0.19}Sb_{0.81}$ pin homojunction lattice matched to GaSb in a back-illumination geometry.

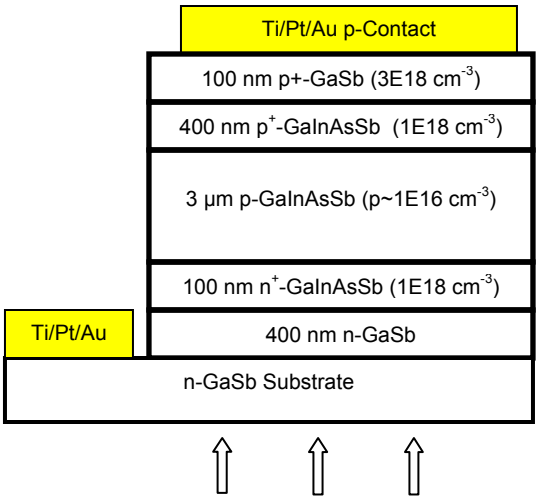

Fig. 3 A p+pn homojunction capped with GaSb and latticed-matched to an n-GaSb substrate. In this back-illuminated geometry, light passes through the substrate and the thin n+ type region before being absorbed in the p-absorbing region. The thick GaSb cap layer can both protect the homojunction during processing as well as block minority carriers from reaching the surface, where nonradiative recombination can be rapid.

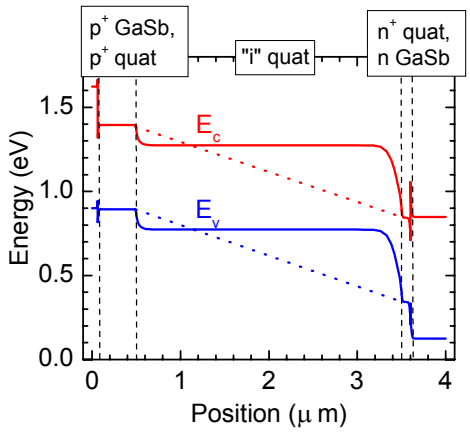

Fig. 4 The calculated real space energy bandstructure (solid lines) of the p+pn+ quaternary diode shown in Fig. 3. Calculations were performed with a one-dimensional diode simulation program. The effect of the background p-doping is to squash the depletion region up against the n-interface. In a true pin structure, the depletion region would stretch across the entire i-region (dashed lines).

2. THEORTICAL BACKGROUND

Some general expectations can be formed for the dependence of the R_0A of a p+pn+ structure, which can be idealized as a pn+ structure, on the background doping level of the absorbing region by inspection of the usual analytical expressions for the diffusion and generation-recombination current in a pn junction (SI units):

$$J_{diff} = n_i^2(T)\sqrt{ek_BT}\left(\frac{1}{N_A}\sqrt{\frac{\mu_e}{\tau_e}} + \frac{1}{N_D}\sqrt{\frac{\mu_h}{\tau_h}}\right)\left(\exp(eV/k_BT) - 1\right) \quad (1)$$

$$J_{GR} = \frac{-en_i(T)d(V)}{\tau_{GR}}\frac{\sinh(-eV/2k_BT)}{e(V_{bi}-V)/2k_BT}f(b) \quad (2)$$

where $n_i(T)$ is the temperature-dependent intrinsic carrier concentration, e is the electron charge, k_B is Boltzman's constant, T is temperature, N_A and N_D are the acceptor and donor densities in the p and n+ regions, respectively; μ_e, τ_e, and μ_h, τ_h are the mobility and lifetime of electrons and holes, respectively; V is the bias voltage and V_{bi} the built in potential; τ_{GR} is the generation recombination lifetime; E_g is the bandgap, $\hbar$ is Planck's constant; d(V) is the depletion width;

$$f(b) = \int_0^\infty \frac{du}{u^2 + 2bu + 1}, \; b = \exp\left(-\frac{eV}{2k_B T}\right). \tag{3}$$

and the width of the depletion layer is:

$$d(V) = \left[\frac{(N_D / N_A)}{N_D + N_A}\left[\frac{\varepsilon(V_{bi} - V)}{2\pi e}\right]\right]^{1/2}. \tag{4}$$

with ε the permittivity. Equations (1) and (2) show that the generation-recombination current is directly proportional to the width of the depletion region, while the diffusion current is independent of the depletion region width. Equation (4) shows that the width of the depletion region is very sensitive to the background doping levels N_A of the p-type absorbing region. Thus in materials that are generation-recombination limited, the expectation is that a narrower depletion region should improve R_0A by reducing the generation-recombination current. Due to the relatively short generation-recombination times in GaInAsSb materials, the general expectation is that device performance will be limited by generation-recombination and not diffusion currents. The trade-off to increasing the p-doping density of the absorbing region is that the narrowing of the depletion region accompanied by a decreasing electron diffusion length will lead to a steady decrease in the device responsivity.

These general expectations are born out more quantitatively in Figs. 5 and 6, which show a simulation of resistivity and responsivity versus doping of the absorbing region of the structure in Fig. 3 as carried out by a one-dimensional diode program. Parameters used in the model were: τ_{SHR} = 10 ns (Shockley-Read-Hall lifetime for electrons and holes), B_{rad} = $5x10^{-11}$ $cm^{-3}s^{-1}$ (radiative recombination coefficient), C_{Auger} = $3x10^{-27}$ $cm^{-6}s^{-1}$ (Auger scattering coefficient), μ_h=300 cm^2/Vs, μ_e=3000 cm^2/Vs, m_h=0.32m_0, m_e = 0.039m_0 (hole and electron mobility and effective mass, respectively, with m_0 the free electron mass), n = 3.75 (index of refraction), and E_g = 501 meV (quaternary bandgap) for the dynamic resistance and additionally α = 4590 cm^{-1} (absorption coefficient) at λ=2.30 μm for responsivity. To determine whether

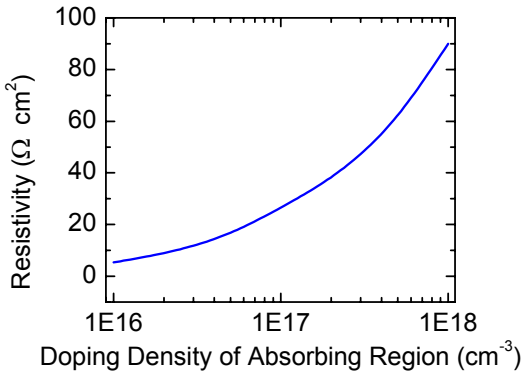

Fig. 5 Simulation by a one-dimesional diode program of the structure in Fig. 3 shows an increase in resistivity versus p-doping of the absorbing region.

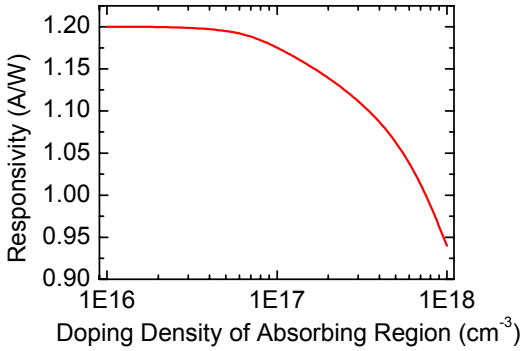

Fig. 6 Simulation by a one-dimesional diode program of the structure in Fig. 3 shows a decrease in responsivity versus p-doping of the absorbing region.

there is an overall improvement or not in the performance of the diode, D* is plotted in Fig. 7 versus doping of the absorbing region. There is a steady increase in D* as the structure of Fig. 3 goes from a p+pn+ junction to a p+n+ junction. The improvements in R_0A thus outweigh the decrease in responsivity to give an overall improvement in D* in pn structure compared to a pin structure.

To test the conclusions of the theory, we grew, processed and characterized a series of five structures with doping of the absorbing region varying so the structure transitions from p+pn+ to p+n+.

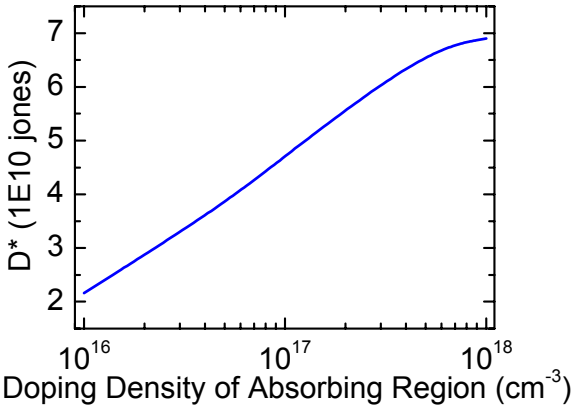

Fig. 9 Simulation of D* of the structure in Fig. 3 shows a steady increase in D* as the doping density of the absorbing region is increased so the structure transitions from p+pn+ to p+n+. Simulations are performed with a one dimensional diode program.

3. MBE GROWTH

All samples for this study were grown in a Veeco-Applied Epi 930 molecular beam epitaxial system equipped with valved crackers for the group V materials Sb and As, and dual filament SUMO cells for the group III materials In and Ga. Sb and As cracking zones were held at 1000 ºC and 900 ºC, respectively, yielding monomeric Sb and As_2. GaInAsSb quaternary materials were grown on a p-type, (100)-oriented GaSb substrates 500 microns thick. Substrates were etched for 1 minute in concentrated HCl to thin the oxide layer along with pre- and post- degreasing steps, which we have found leads to improved post epi-growth surfaces, consistent with previous studies.[3] Substrates were first outgassed in the intro chamber for 2 hours at 175 ºC, 1 hour at 350 ºC (thermocouple temperature) in the buffer chamber, and then the oxide layer was thermally desorbed in the growth chamber under an Sb beam equivalent pressure (BEP) flux of 7×10^{-7} Torr. After the onset of desorption at about 495 ºC according to an optical pyrometer, the substrate was heated to 515 ºC for 10 minutes to ensure full removal of the oxide layer across the substrate. The optical pyrometer was calibrated with respect to a 1×3 to 1×5 reflection high energy electron diffraction (RHEED) pattern transition, which was observed to occur at 400 ºC under a monomeric Sb BEP flux of 7×10^{-7} Torr.

Before growing device structures, the quaternary growth was optimized to give a quaternary with 2.37 μm cut off wavelength and latticed matched to the GaSb substrate. According to the plot in Fig. 1, the material composition of such an epilayer is $Ga_{0.80}In_{0.20}As_{0.18}Sb_{0.82}$. To set the Ga concentration x=0.80, the Ga and In cell temperatures were chosen such that $R_{GaSb}/(R_{GaSb}+R_{InAs}) = x$. The total V/III beam equivalent pressure (BEP) flux ratio was about 3, chosen to be as close as possible to stoichiometric growth conditions. Lattice-matching was achieved by growing a series of quaternary structures varying only the As_2 flux. The lattice match was checked with a high resolution x-ray diffraction (HRXRD) measurement. Figure 10 shows the lattice match of the quaternary series as a function As_2 BEP flux. The inset to Fig. 10 shows an example HRXRD measurement. The peak separation Δθ of the GaSb substrate (peak at 0 arcsec) and the GaInAsSb alloy can be used to calculate the lattice mismatch using Bragg's Law: $(L_{GaSb}-L_{GaInAsSb})/L_{GaSb} = 8\times10^{-6}$ arcsec^{-1} Δθ. Using this method, a lattice mismatch of less that 10^{-4} was achieved. The cutoff wavelength was determined with a room temperature photoluminescence measurement, shown in Fig. 11 to be 2.37 μms for the samples grown in this study.

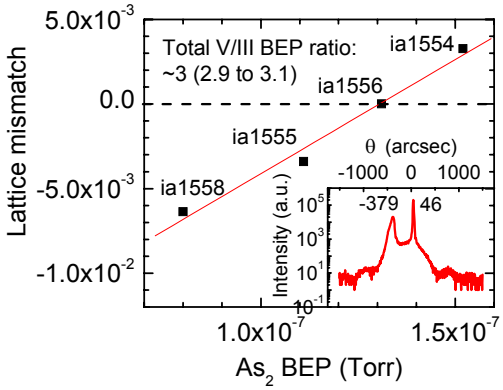

Fig. 10 Lattice mismatch of the GaInAsSb quaternary material to the GaSb substrate as a function of the As_2 BEP flux. The lattice mismatch scales approximately linearly with increasing As_2 flux. The inset shows a sample high-resolution x-ray diffraction measurement.

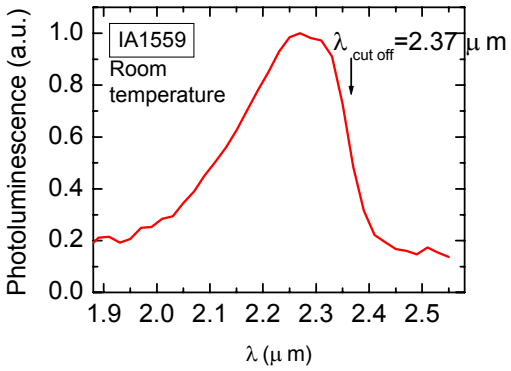

Fig. 11 A room temperature photoluminescence measurement of the lattice-matched quaternary used to grow the device structures of Fig. 3.

4. DEVICE PROCESSING AND CHARACTERIZATION

Processing was begun by photolithography to define sets of variable sized rectangular mesas followed by wet etching. The optimized etch chemistry was [Citric Acid : H_3PO_4 : H_2O_2] and resulted in a step-like profile to a depth just beyond the total thickness of the device structure into the substrate. A photoresist was then deposited on the mesas, and photolithography was used to remove photoresist from the tops of the mesas for p-metal contacts and a portion of the etched surface for n-metal contacts. After an oxygen plasma etch and a dip in hydrochloric acid and ammonium sulfide to clean contact areas, Ti/Pt/Au was deposited in a single step to form both the n- and p-metal contacts. The I-V measurements were performed on two mesa sets for each sample at room temperature using a Hewlett Packard 4155A semiconductor parameter analyzer.

5. EXPERIMENTAL RESULTS AND DISCUSSION

In order to compare the intrinsic R_0A of each of the detectors in the series, a simple model was used to disentangle intrinsic junction performance from perimeter leakage effects. The mesa diode can be viewed as consisting of two resistors in parallel, an areal resistor R_{diode} and an edge resistor R_{edge}. Then the total diode resistance can be calculated:

$$\frac{1}{R_0 A} = \frac{1}{R_{diode} A} + \frac{1}{R_{edge} A}. \tag{7}$$

$R_{diode}A$ is independent of area, while $R_{edge}L$ should be independent of perimeter length L, and hence $1/R_{edge}A$ should increase linearly with perimeter-to-area ratio:

$$\frac{1}{R_0 A} = \frac{1}{R_{diode} A} + m\frac{L}{A} \tag{8}$$

where $m=(R_{edge}L)^{-1}$ is a constant. Equation 8 is then the equation of a straight line with the maximum attainable R_0A one over the y-intercept (i.e. limit of infinite mesa radius). Figure 12 shows a plot of $1/R_0A$ versus perimeter-to-area ratio. A least squares regression analysis gives a best value for R_0A in the zero perimeter to area limit of 97 Ω-cm^2, or a range of 50-500 Ω-cm^2 including uncertainty. The maximum R_0A for the largest 1 mm^2 mesa was 30 Ω-cm^2.

Using the above analysis on all detectors in the series, we obtained a summary plot of R_0A in the zero perimeter to area limit in Fig. 13. Within uncertainty, little difference is seen in the R_0A of all samples grown in the series. The deviation of the experimental results from the expected trend from theoretical simulations in Fig. 5 is not yet understood, and will require further investigation. Here, we offer a couple of tentative explanations. One is that the samples are not limited

by generation-recombination currents but by diffusion currents. As discussed in the theoretical background, the improvement in R_0A seen in Fig. 5 is not expected for a detector in a diffusion limit. Another explanation is that the decreases in the generation-recombination current expected from increasing the doping density of the absorbing region were erased by a decreasing generation-recombination time, which was assumed constant in the theoretical simulations in Sec. 2. This could happen due to deteriorating material quality with increasing doping. To further investigate these tentative explanations, we plan temperature dependent measurements of the I-V characteristics of the samples, followed by quantitative analysis of the I-V curves. We also plan to measure the responsivity of each sample.

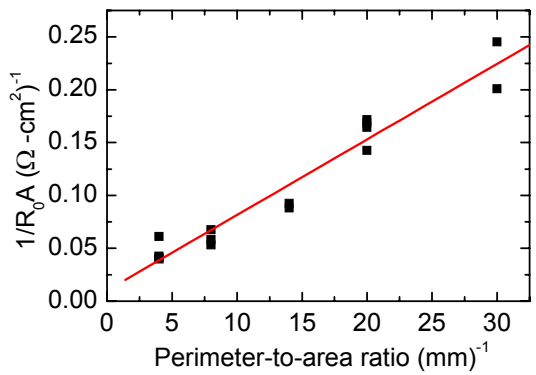

Fig. 12 A plot of the experimentally measured $1/R_0A$ versus perimeter-to-area ratio for the detector structure ia1560 gives a linear relationship that allows extraction of R_0A in the zero-perimeter limit using a least squares regression analysis.

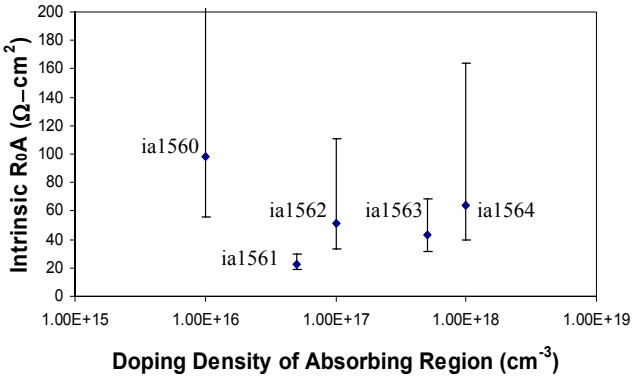

Fig. 13 Summary plot of the experimental R_0A in the zero perimeter limit as a function of the doping density of the absorbing region.

6. CONCLUSIONS

A theoretical investigation of pin versus pn junctions from materials limited by generation-recombination currents suggests that pn junctions should have a better D* than pin junctions. A series of p+pn+ junctions were grown with a variation in the doping of the absorbing region to give detectors ranging from p+pn+ to p+n+ to test this hypothesis. Within uncertainty, no clear trend was seen in the R_0A of the devices. A technique to separate out perimeter leakage effects from junction performance was presented. The maximum measured R_0A was 30 Ω-cm^2 for our quaternary p+pn+ structures, and the maximum extracted junction R_0A in zero perimeter to area limit was 100 Ω-cm^2.

ACKNOWLEDGEMENT

This work was supported by the NIH under contract number DK-02925.

7. REFERENCES

[1] I. Vurgaftman, J.R. Meyer, L.R. Ram-Mohan, "Band parameters for III-V compound semiconductors and their alloys," J. of Appl. Physics **89**, 5815 (2001).

[2] M.H.M. Reddy, J.T. Olesberg, C. Cao, J.P. Prineas, "MBE-grown high-efficiency GaInAsSb mid-infrared detectors operating under back illumination," Semiconductor Sci. Technol. **21**, 267-72.

[3] C.J. Vineis, C.A. Wang, K.F. Jensen, "In-situ reflectanc monitoring of GaSb substrate oxide desorption," J. of Cryst. Growth **225**, 420 (2001).